Influence of CBCT parameters on the output of an automatic edge-detection-based endodontic segmentation

Jérôme Michetti, Marie Georgelin-Gurgel, Jean-Philippe Mallet, Franck Diemer, Kader Boulanouar

Dentomaxillofacial Radiology (2015) 44, 20140413

birpublications.org/dmfr

RESEARCH ARTICLE

Influence of CBCT parameters on the output of an automatic edge-detection-based endodontic segmentation

[1,2]J Michetti, [1,3]M Georgelin-Gurgel, [1]J-P Mallet, [1,4]F Diemer and [2]K Boulanouar

[1]*Faculté de Chirurgie Dentaire, Université Paul Sabatier, Centre Hospitalier Universitaire, Toulouse, France;* [2]*Laboratoire INSERM, Imagerie Cérébrale et Handicaps Neurologiques UMR 825, Centre Hospitalier Universitaire, Toulouse, France;* [3]*Laboratoire des Déficiences, Incapacités et Désavantages en Santé Orale, EA4847, Université d'Auvergne, Clermont-Ferrand, France;* [4]*Group SUMO, Institut Clément Ader, Toulouse, France*

Objectives: To determine the optimal CBCT settings for an automatic edge-detection-based endodontic segmentation procedure by assessing the accuracy of the root canal measurements.
Methods: 12 intact teeth with closed apexes were cut perpendicular to the root axis, at predetermined levels to the reference plane (the first section made before acquisition). Acquisitions of each specimen were performed with Kodak 9000® 3D (76 μm, 14 bits; Kodak Carestream Health, Trophy, France) by using different combinations of milliamperes and kilovolts. Three-dimensional images were displayed and root canals were segmented with the MeVisLab software (edge-detection-based method; MeVis Research, Bremen, Germany). Histological root canal sections were then digitized with a 0.5- to 1.0-μm resolution and compared with equivalent two-dimensional cone-beam reconstructions for each pair of settings using the Pearson correlation coefficient, regression analysis and Bland–Altman method for the canal area and Feret's diameter. After a ranking process, a Wilcoxon paired test was carried out to compare the pair of settings.
Results: The best pair of acquisition settings was 3.2 mA/60 kV. Significant differences were found between 3.2 mA/60 kV and other settings ($p < 0.05$) for the root canal area and for Feret's diameter.
Conclusions: The quantitative analyses of the root canal system with the edge-detection-based method could depend on acquisition parameters. Improvements in segmentation still need to be carried out to ensure the quality of the reconstructions when we have to deal with closer outlines and because of the low spatial resolution.
Dentomaxillofacial Radiology (2015) **44**, 20140413. doi: 10.1259/dmfr.20140413

Cite this article as: Michetti J, Georgelin-Gurgel M, Mallet J-P, Diemer F, Boulanouar K. Influence of CBCT parameters on the output of an automatic edge-detection-based endodontic segmentation. *Dentomaxillofac Radiol* 2015; **44**: 20140413.

Keywords: cone-beam computed tomography; radiographic image enhancement; endodontics; image processing; root canal

Introduction

In endodontics, a good knowledge of the root canal anatomy is an indispensable pre-requisite to ensure treatment success. Three guidelines are important: to identify and prepare the main canals, to establish and respect working lengths and to assess the initial apical canal diameter in order to allow an adequate preparation size.[1] Many tools to measure root canal anatomy have been developed with micro-CT. Given the high spatial resolution provided by these devices, a simple thresholding is sufficient to extract and analyse the root canal system. However, owing to the limitation of the field of view (only small samples or extracted teeth can be studied) and the radiation dose, micro-CT is not

Correspondence to: Dr Jerome Michetti. E-mail: jerome.michetti@gmail.com
Received 2 December 2014; revised 22 May 2015; accepted 1 June 2015

suitable for clinical use.[1] Nowadays, except micro-CT, there is no CBCT application dedicated to endodontics and aimed at exploring the root canal system quantitatively to help clinicians in their treatments. CBCT is an extraoral imaging system dedicated to explore the whole maxillofacial region or to partially explore dentomaxillofacial structures (field of view varies from 15 to 5 cm or less).[2] Spatial resolution depends on the field of view used and, in general, a smaller scan volume corresponds to a higher spatial resolution of the image (the resolution varies from 0.600 to 0.075 mm).[3] Recently, CBCT was described as an interesting endodontic measurement tool because high correlation was found between histological sections and CBCT-equivalent images.[4] Quantitative analysis of the root canal requires segmentation of the endodontic system owing to the limitation of the quality of the CBCT scans (low resolution and short size of the root canal anatomy). Image segmentation is a post-processing method to split images into homogeneous parts (in our case, to separate the endodontic system from the surrounding tissue, the dentine). It is typically used to locate and analyse objects and boundaries (lines, curves etc.) in images.[5] Volumetric assessment of an object with manual segmentation of its outlines is a time-consuming process and can be overcome with the help of computerized segmentation methods.[6,7] In the automatic segmentation process, each of the pixels in a region is similar with respect to some characteristic or computed property. Adjacent regions are significantly different with respect to the same characteristic(s).[5] When applied to a stack of images, typical in medical imaging, the resulting contours after image segmentation can be used to create three-dimensional (3D) reconstructions.[8] The choice of an appropriate segmentation technique is important owing to its influence on morphometric parameters.[9,10] The main difficulties in automatic medical image segmentation are the lack of spatial resolution and contrast of images. For this reason, an ideal segmentation method does not exist. There are many techniques (thresholding, deformable boundary-based methods, region growing, edge detection etc.), which can be used separately or combined. Several segmentation methods can be carried out for the same image; a good segmentation is the one that allows a good interpretation by simplifying the image without reducing its contents.[5]

Segmentation results depend on the image to be studied, and, consequently, acquisition settings have an influence on the reconstruction quality.[11] An increase in milliamperes leads to an increase of not only the signal-to-noise ratio but also the radiation dose. An increase in kilovolts increases the average photon energy and decreases the greyscale resolution.[12] The choice of acquisition settings could affect automatic segmentation procedures.[9]

The aim of this study was to assess the influence of acquisition parameters on an automatic edge-detection-based segmentation procedure in order to ensure the most accurate measurements of the root canal anatomy. For validation purposes, CBCT two-dimensional (2D) segmented endodontic reconstructions from different acquisition settings were compared with equivalent histological root canal contours.

Methods and materials

Specimen preparation, section and digitization

12 different intact freshly extracted teeth (1 maxillary incisor, 1 mandibular incisor, 1 maxillary canine, 1 mandibular canine, 2 maxillary premolars, 2 mandibular premolars, 2 maxillary molars and 2 mandibular molars) with closed apices were selected. These teeth were an anonymous donation for research purposes. The roots of each specimen were embedded in a photoelasticimetry clear plastic cuvette (Kartell spa, Noviglio, Italy) with synolite resin (Gaches Chimie Spécialités, Toulouse, France) up to the cementoenamel junction. Using a specimen holder suited to the shape of the prefabricated container, each specimen was fixed in a precise, reproducible way onto the moving arm of a small cut-off machine (diamond disk, 12.7: 100×0.3 mm; Asahi Diamond Industrial Europe SAS, Chartres, France).[2] This device ensured an identical specimen position at each step of the protocol and that all sections were cut in the same plane. From each tooth, 10 histological slices were cut perpendicular to the root axis, at pre-defined levels parallel to the reference plane, which was taken as the first and most coronal section. In order to use this plane as a reference plane for both the CBCT images and the histological images, we cut this plane before CBCT acquisition.

The dimension of the root canal of the coronal and apical sides of each histological slice was measured after digitization under an optical microscope (BX51M; Olympus, Tokyo, Japan) by using a camera (U-CMAD3/DP20; Olympus). Magnifications of $\times 5$ or $\times 10$ were chosen according to the canal size, so that the whole contour was visible with the best resolution (0.5 or 1.0 μm). We excluded histological sections when the outline of the canal was too large to fit into the field of view of the optical microscope.

Root canal contours were selected manually by using the "polygon selections" function of the image processing and analysis software (ImageJ 1.45b; National Institutes of Health, Bethesda, MD). Two values were computed: cross-sectional area of the root canal lumen and Feret's diameter, which defines the longest distance between two parallel straight lines that are tangents to the shape (Figure 1).

CBCT acquisition, reconstruction and segmentation

Once the coronal section had been made, acquisitions of each specimen were performed by CBCT with the Kodak 9000® 3D (Kodak Carestream Health, Trophy, France). Each sample was placed in the centre of the cone beam. After a single rotation, this acquisition system reconstructs a volume with a spatial resolution of 76 μm (isotropic voxel) and a grey value range of 14 bits.

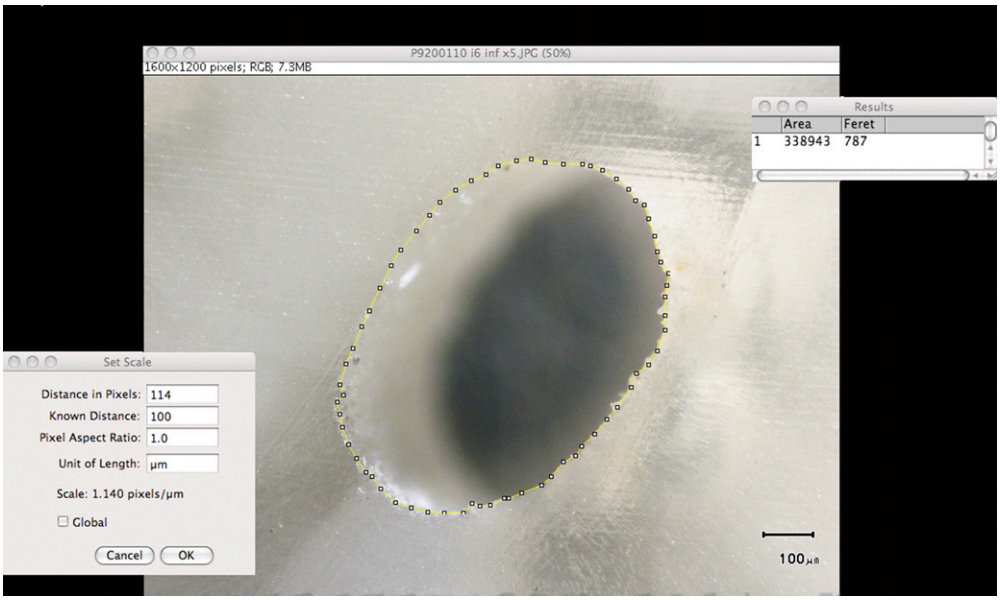

Figure 1 Root canal contour selection on ImageJ (National Institutes of Health, Bethesda, MD) and measurement of area and Feret's diameter after setting scale.

Different combinations of milliamperes and kilovolts were used for each sample: 2.0, 2.5, 3.2, 4, 5 and 6.3 mA at 60, 65 and 70 kV. Consequently, 15 combinations of settings were used to reconstruct each tooth. The position of the sample was unchanged during the 15 image acquisitions. Then, a new sample underwent CBCT and 15 other acquisitions were performed.

From each acquisition, 2D projections were collected during the sweep around the tooth. 3D representation of the sample was reconstructed from the 2D projections with the KDIS® software v. 3.8 (Kodak Carestream Health, Trophy, France), provided with the 9000 3D. The algorithm of reconstruction of this software builds the volume and saves it in digital imaging and communications in medicine format. These volumetric datasets can be studied by using different representations (multiplanar reformation, 3D surface rendering) provided by the visualization toolkit of the KDIS software.

Digital imaging and communications in medicine data (volumes) were moved to the MeVisLab image processing and visualization platform (MeVis Research, Bremen, Germany) to launch the root canal segmentation procedure, which extracts the relevant information from the images. Before segmentation, each volume was moved to make every 2D transverse canal reconstruction parallel to the reference section and so too to the histological sections. This procedure corresponds to a rigid registration with six degrees of freedom (only rotations were used to bring the volume into registration).[13] The segmentation framework used was based on the "canny edge detection", which seems to satisfy the constraints of good sensitivity, localization and noise robustness (Figure 2). We should note that this segmentation procedure does not directly depend on the intensity values of the voxels but is based on the spatial gradient operation able to highlight brightness discontinuities. It provided us with a binary image where each pixel is marked as either a root/canal edge pixel or non-edge pixel. In order to close the root canal space, we applied a closing morphological procedure that consisted of dilatation followed by erosion (Figure 3). Dilatation enabled us to fill small background holes in binary images but involved distortion in all regions of the object pixels. To reduce this effect, erosion with the

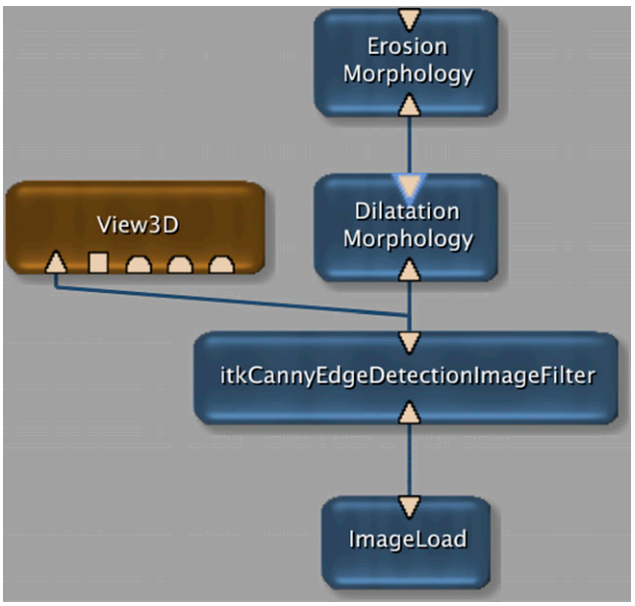

Figure 2 MeVisLab (MeVis Research, Bremen, Germany) customized framework for edge detection and closing morphological procedure. 3D, three dimensional.

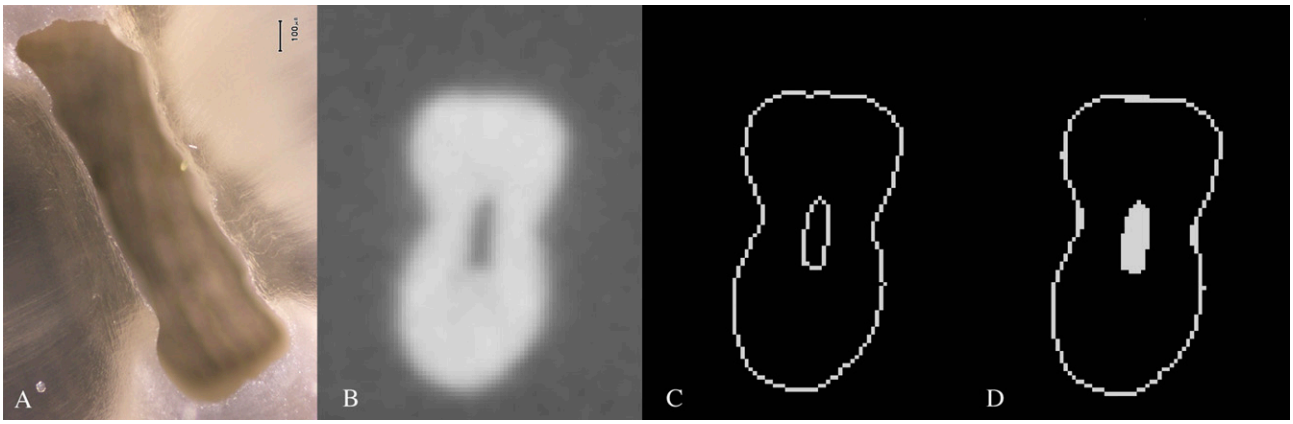

Figure 3 Comparison between the histological section and pre-, per-, and post-CBCT-equivalent section for a maxillary premolar. (a) Histological slice. (b) Initial two-dimensional reformatted image. (c) Root canal segmentation result. (d) Closing morphological procedure result.

same structuring element was performed. In our study, the structure element was a kernel $13 \times 13 \times 13$ voxels.

Afterwards the files were moved to ImageJ to allow canal measurements on the CBCT 2D reconstructions by using the "Wand (tracing) tool" function, in the same way we did for the histological sections (Figure 4).

Statistical analysis

The accuracy of the measurements of the root canal in the CBCT image was evaluated by comparing with the real measurements of this anatomy from the histological sections. The histological and CBCT results were compared using two different measurements, the canal area and the Feret's diameter. The comparison was based on Pearson correlation analysis (r) (to show the potential linear relationships between the measurements), on linear regression analysis (slope and intercept) and, for assessing the degree of agreement between the two techniques, on the calculation of the bias (mean of differences between the two estimated sets).

A ranking process by using criteria of comparison was performed to obtain a classification of the acquisition settings in increasing order, that is, from the best pair to the worst one.

To evaluate if the best settings allow a significant improvement compared with the others, the non-parametric Wilcoxon paired test compared CBCT measurements of each pair. The level of significance was set at 5% ($p \leq 0.05$).

Results

One of the teeth could not be included in the results owing to a defect of resin embedding. From the 11 remaining teeth (17 canals), 243 sections were compared for each pair of settings.

In order to work on a statistically relevant data set, we combined measurements of the different teeth for the root canal area and for Feret's diameter.

With the 15 pairs for the area, we found a coefficient of correlation of 0.75 (0.67 for the worst pair to 0.81 for the best) and an underestimation of CBCT measurements as compared with the histological areas: $-24\,839\ \mu m^2$ ($-44\,965$ to -6251). Taking into account the pixel size in CBCT acquisitions, the bias of the measurements corresponds on average to 4 pixels. The regression analysis provided a slope of 0.73 (0.60 to 0.80) and an intercept of 24 996 (41 260 to 14 320), as shown in Table 1.

On average, for the Feret's diameter, the correlation coefficient was -0.71 (0.58 for the worst pair to 0.80 for the best). The mean of the differences was $-42\ \mu m$ (-84.09 to -0.89), which also indicates an underestimation of CBCT and represents on average a bias in CBCT pixels of less than 1 pixel. The slope ranged between 0.54 and 0.84 with a mean of 0.70, while the intercept found was 148.29 (219.41 to 78.47), as highlighted in Table 2.

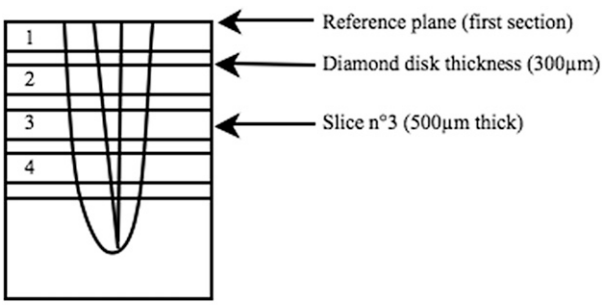

a

Slice		CBCT	
N°1: apical side	500µm	532µm	7 voxels
N°2: coronal side	800µm	836µm	11 voxels
N°2: apical side	1300µm	1292µm	17 voxels
N°3: coronal side	1600µm	1596µm	21 voxels
N°3: apical side	2100µm	2128µm	28 voxels

b

Figure 4 (a) Pre-determined levels for histological sections. (b) Correspondence with two-dimensional CBCT reconstructions.

Table 1 Results for root canal area

	Pairs of settings												
Area	*2 mA 60 kV*	*2 mA 65 kV*	*2.5 mA 60 kV*	*2 mA 70 kV*	*2.5 mA 65 kV*	*3.2 mA 60 kV*	*2.5 mA 70 kV*	*3.2 mA 65 kV*	*4 mA 60 kV*	*3.2 mA 70 kV*	*4 mA 65 kV*	*5 mA 60 kV*	*4 mA 70 kV*	*5 mA 65 kV*	*6.3 mA 60 kV*
CC (r)	0.67	0.70	0.76	0.74	0.77	0.79	0.75	0.77	0.74	0.74	0.75	0.77	0.68	0.78	0.81
p-value	1.02E-32	8.15E-38	7.65E-48	1.13E-43	1.27E-49	8.52E-54	1.90E-44	4.24E-49	4.80E-43	1.18E-42	6.50E-46	4.40E-49	4.23E-34	1.39E-51	2.97E-57
MD (μm^2)	−6251	−15 996	−6708	−33 770	−20 964	−20 239	−39 974	−25 338	−16 204	−39 754	−25 944	−21 861	−44 965	−30 941	−23 674
SD	115 262	102 459	93 209	91 730	88 681	85 352	91 283	88 456	96 202	92 449	92 106	89 624	101 384	86 032	81 566
Slope	0.75	0.71	0.80	0.68	0.76	0.79	0.69	0.75	0.74	0.66	0.74	0.77	0.60	0.76	0.80
95% CI	0.64 to 0.85	0.62 to 0.80	0.71 to 0.88	0.60 to 0.75	0.68 to 0.84	0.72 to 0.97	0.61 to 0.76	0.67 to 0.83	0.66 to 0.83	0.59 to 0.74	0.66 to 0.82	0.69 to 0.85	0.52 to 0.69	0.68 to 0.83	0.72 to 0.87
Intercept	41 260	37 518	30 847	26 737	23 169	18 164	18 387	21 850	32 052	23 121	22 595	21 382	28 983	14 320	14 549
95% CI	17 246 to 65 274	16 786 to 58 250	11 387 to 50 307	9079 to 44 395	5093 to 41 245	542 to 35 786	666 to 36 108	4013 to 39 687	12 466 to 51 639	5483 to 40 759	3985 to 41 205	3036 to 39 728	10 088 to 47 879	−3068 to 31 708	−2210 to 31 309

CC, Pearson's correlation coefficient; CI, confidence interval; MD, mean of differences; SD, standard deviation.

For extracted teeth, root canal edge-detection-based segmentation provides the best results when using the combination of the settings 3.2 mA and 60 kV (Table 3). A strong correlation coefficient was found between CBCT and histological sections for area (0.79, $p < 0.001$) and Feret's diameter (0.79, $p < 0.001$). The degree of agreement with the Bland–Altman method indicates that the results were not graphically different for the two measurements: $-20\,239\ \mu m^2 \pm 85\,352$ (95% confidence interval, −187 529 to 147 051) for the area and −35.83 μm ± 214 (95% confidence interval, −456 to 384) for the diameter. The CBCT underestimation represents −11.8% for the area and −3.6% for Feret's diameter.

The Wilcoxon paired test was used as the data were found to be non-gaussian. Statistically significant differences were shown between measurements from this best pair and the other settings (Wilcoxon test, $p < 0.05$) (Table 3).

Discussion

In this study, we used a quantitative assessment of the root canal in order to evaluate the influence of image acquisition settings on an edge-based endodontic segmentation. The aim in radiology is to obtain images adequate for clinical purpose and with the minimum radiation dose (as low as reasonably achievable). The evaluation of imaging performance may depend on the study of clinical images (subjective assessment with scoring of quality criteria) and/or on the use of test objects.[12,14–16] CBCT is described as an efficient 3D imaging system, making it possible as an accurate representation of the root canal system.[3] The interest of our study is to use extracted teeth as test objects, which allow us to perform an objective assessment of the quality of the CBCT reconstructions with a link to the clinical needs to measure the root canal anatomy.

The enhancement in image quality could be obtained by using more radiant techniques. Therefore, it is interesting to determine, for a required image quality with a specific imaging system, the loss of clinical information owing to the use of other radiation exposures.[15] The CBCT used in our protocol enables different setting values: 2–15 mA and 60–90 kV. Although the signal-to-noise ratio increases when current and voltage increase, we did not exceed 6.3 mA and 70 kV. Beyond these values, owing to an *in vitro* protocol and to a small volume to explore, complementary metal oxide semi-conductor sensors were overexposed and star artefacts appeared on the reconstructed images. Based upon the specific CBCT used in this study, 3.2 mA and 60 kV seem to provide the best measurements of the root canal anatomy. The best result was compared with the other pairs using the Wilcoxon test (paired samples) and showed statistically significant differences (17 out of the 28 comparisons). Tube voltage exceeding 65 kV provided mostly significant differences on root canal measurements (seven out of the eight),

Table 2 Results for Feret's diameter

	Pairs of settings											
Feret's diameter	*2 mA 60 kV*	*2 mA 65 kV*	*2.5 mA 60 kV*	*2 mA 70 kV*	*2.5 mA 65 kV*	*3.2 mA 60 kV*	*2.5 mA 70 kV*	*3.2 mA 65 kV*	*4 mA 60 kV*	*3.2 mA 70 kV*	*4 mA 65 kV*	*5 mA 60 kV*	*4 mA 70 kV*	*5 mA 65 kV*	*6.3 mA 60 kV*
CC (r)	0.68	0.70	0.77	0.63	0.75	0.79	0.66	0.74	0.80	0.58	0.69	0.79	0.61	0.75	0.75
p-value	7.35E-35	3.62E-37	1.86E-49	2.97E-28	5.62E-46	1.62E-52	1.78E-31	8.36E-43	4.07E-55	8.63E-23	1.22E-35	5.29E-54	1.43E-26	1.69E-44	8.56E-46
MD (μm)	−7.42	−17.80	−0.89	−68.56	−29.88	−35.83	−82.37	−38.91	−23.11	−74.90	−40.30	−35.91	−84.09	−57.02	−38.44
SD	265	257	225	276	229	214	263	237	215	295	258	211	279	237	226
Slope	0.69	0.71	0.79	0.59	0.74	0.78	0.60	0.72	0.84	0.54	0.68	0.79	0.56	0.76	0.71
95% CI	0.60 to 0.79	0.62 to 0.80	0.71 to 0.87	0.50 to 0.68	0.66 to 0.82	0.70 to 0.86	0.51 to 0.69	0.64 to 0.80	0.76 to 0.92	0.44 to 0.63	0.59 to 0.77	0.71 to 0.86	0.47 to 0.65	0.67 to 0.85	0.63 to 0.79
Intercept	187	168	133	191	136	105	171	139	78	219	163	98	194	95	146
95% CI	120 to 253	104 to 233	75 to 192	126 to 257	78 to 194	50 to 159	109 to 233	79 to 199	21 to 136	151 to 288	98 to 227	44 to 153	129 to 259	34 to 156	90 to 201

CC, Pearson's correlation coefficient; CI, confidence interval; MD, mean of differences; SD, standard deviation.

which could be a consequence of an overexposure of the samples. Low-dose protocols presented less significant differences (one of two comparisons and two of three for high-dose protocols). Our results differ from those of Panmekiate et al.[17] On mandibular linear measurements, no significant differences in the distances were found between the different combinations of peak voltage and milliamperes. Using a human mandible cadaver, Hassan et al[14] showed CBCT scan mode (exposure time) was less relevant on root canal visibility. Kwong et al[12] evaluated subjectively the image quality of head skull CBCT by varying settings (mA and kV) and fields of view. Variation of voltage did not change the image quality, and the use of lower tube currents enabled good diagnostic quality. On the other hand, Gündoğdu et al[18] with the analysis of adult cranial CT in 60 patients observed significant differences not only between standard and low-dose protocols but also between low-dose protocols. In our study, the root canal visibility does not seem to ensure an accurate measurement of its anatomy. The use of segmentation to undergo a quantitative assessment of the endodontic system, which is a necessary step because of the low spatial resolution, appeared to be sensitive to acquisition settings. The best pair obtained for extracted teeth may also deviate from the clinical situation. Our study was limited not only by the absence of surrounding periodontical structures, which involves a high signal-to-noise ratio, but also by the absence of structures placed outside the field of view, which may be a source of certain artefacts.[19]

The requirements in segmentation are important in endodontics owing to the partial volume effect. Segmentation of CT data is not easy, and its complexity is often underestimated.[10] It is a necessary pre-processing step in the accurate quantitative analysis of a small anatomical structure by highlighting its precise boundaries.[20] Outlines should be thin boundary lines reflecting the actual boundary of the original structure. Methods using global thresholds provide more or less successful results: a grey value is chosen as the threshold to separate the object from the background. This technique is easy and quick to apply[21,22] but depends on the amount of noise, the contrast between structures and partial volume effects. A threshold value could be optimal for a certain part of the object but not for the whole.[3,9,10] MeVisLab is a software package for medical images, providing a modular visual programming interface with a comprehensive suite of image processing and visualization tools.[21] An interest of our study was to use the gradient grey value for detection of the root canal outline, which represents the amount of difference between grey values of two neighbouring voxels. It deals with the difference and could be less dependent on grey value variations, which can be found according to the patients or the parameters of acquisition. After segmentation, certain apical canal sections too close to the root surface could not be segmented or involved aberrant diameter and surface measurements. The same excessive results were observed with canal junction or

Table 3 Ranks and results for Wilcoxon paired tests (*p*-value)

	Pairs of settings														
Rank	*2 mA 60 kV*	*2 mA 65 kV*	*2.5 mA 60 kV*	*2 mA 70 kV*	*2.5 mA 65 kV*	*3.2 mA 60 kV*	*2.5 mA 70 kV*	*3.2 mA 65 kV*	*4 mA 60 kV*	*3.2 mA 70 kV*	*4 mA 65 kV*	*5 mA 60 kV*	*4 mA 70 kV*	*5 mA 65 kV*	*6.3 mA 60 kV*
Area															
CC	15	13	7	10	4	**2**	9	5	11	12	8	6	14	3	1
MD	1	3	2	12	6	**5**	14	9	4	13	10	7	15	11	8
Slope	8	11	1	13	5	**3**	12	7	9	14	10	4	15	6	2
Intercept	15	14	12	10	9	**3**	4	6	13	8	7	5	11	1	2
Wilcoxon test	0.0048	NS	0.0001	NS	NS		0.0008	NS	NS	0.0000	0.0027	NS	0.0000	0.0000	0.0333
Feret's diameter															
Pearson's coefficient	11	9	4	13	5	**3**	12	8	1	15	10	2	14	7	6
Mean of differences	2	3	1	12	5	**6**	14	9	4	13	10	7	15	11	8
Slope	10	9	2	13	6	**4**	12	7	1	15	11	3	14	5	8
Intercept	10	9	2	13	6	**4**	12	7	1	15	11	3	14	5	8
Wilcoxon test	0.0095	NS	0.0003	0.0458	NS		0.0026	NS	NS	0.0020	0.0374	NS	0.0000	0.0000	0.0380
Cumulative rank	72	71	31	96	46	**30**	89	58	44	105	77	37	112	49	43
Final rank	10	9	2	13	6	**1**	12	8	5	14	11	3	15	7	4

CC, Pearson's correlation coefficient; MD, mean of differences; NS, not significant.
Best pair results are shown in bold.

separation. Liu et al[23] stressed the fact that the segmentation of a tooth becomes more difficult when it is adjacent to the cortical bone. In our study, this difficulty increased owing to the spatial resolution and to the proximity of different edges. Exclusion and aberrant differences seem also to be owing to the closing morphological operation. This step used to remove the canal involved the junction of outlines, which appeared separated after edge detection.

The comparison for the best pair results showed strong correlations (0.79) between histological and CBCT sections (Figures 5 and 6). With the Bland–Altman analysis, we found relatively equivalent measurements for the diameter (18 sections falling outside the limits of the agreement). The dispersion for the area seems to increase with the size of the section (nine sections were out of the limits of the agreement). Both Feret's diameter and the area presented a slight underestimation for CBCT. Our results seem to be in agreement with those of Liu et al[23] and Michetti et al.[4] With a semi-automated segmentation (magic wand as the region-growing tool) of tooth volume, Liu et al[23] found slight deviations between CBCT and physical volumes. They concluded that *in vivo* determination of tooth volumes

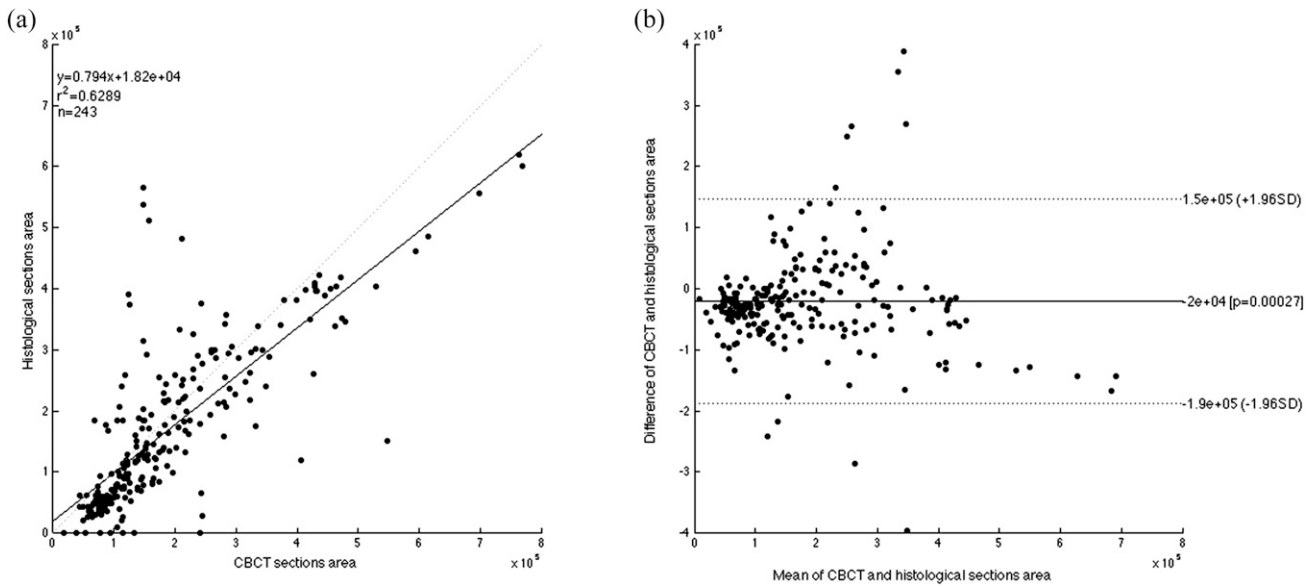

Figure 5 Scatter plot with the regression line of root canal section areas with respect to histological and CBCT sections (a). Bland–Altman plot of area measurements between histological sections and CBCT images. Negative values indicate smaller areas calculated from CBCT than from histological data (b).

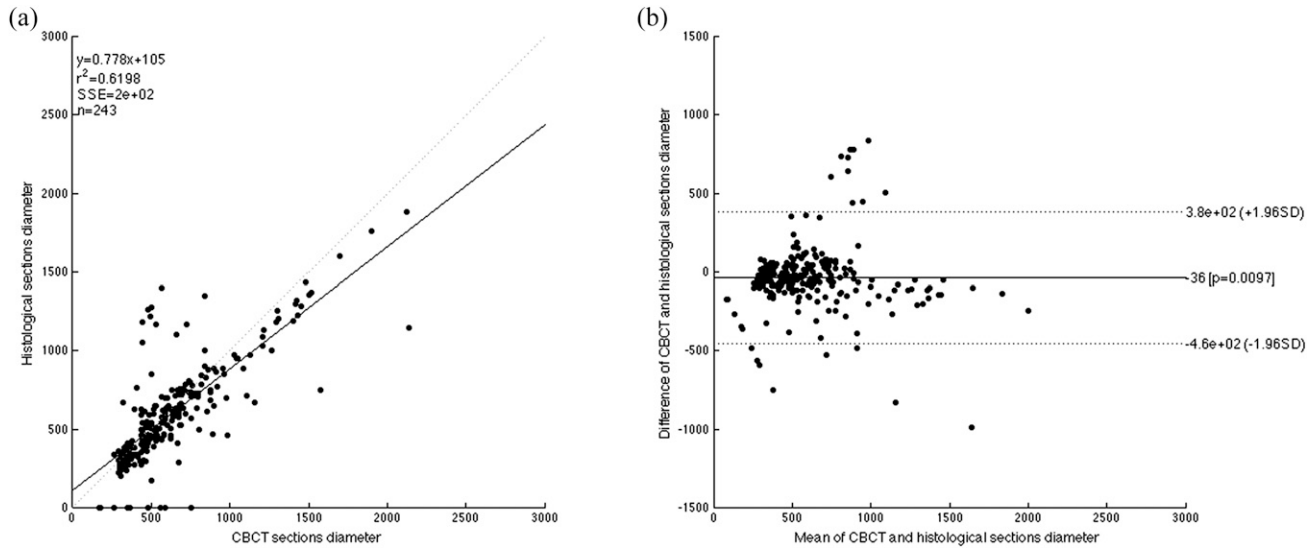

Figure 6 Scatter plots with regression lines of root canal section diameter with respect to histological sections and CBCT images (a). Bland–Altman plot of Feret's diameter measurements between histological sections and CBCT images. Negative values indicate smaller diameters calculated from CBCT than from histological data (b).

from CBCT is feasible. Smoothing operations appeared also to reduce CBCT volume measurements. By using another automatic segmentation on extracted teeth, Michetti et al[4] showed high correlation between CBCT and histological sections of the root canal system. In the same manner, CBCT provided smaller measurements of the anatomy with a bias of $<3\%$.

The CBCT ability to quickly provide good quality three-dimensional images of teeth and of the root canal anatomy might be useful for teaching and for research purposes (Figure 7). Further investigations with *in vivo* conditions or the use of more realistic object tests with extracted teeth are necessary to confirm these results before their use in clinical situations.

Conclusions

CBCT with a resolution of 76 μm and edge-detection-based segmentation seem to provide accurate assessment of the internal anatomy of teeth. Improvements in segmentation still need to be made to ensure the quality of the reconstruction whatever the root canal system found. Nevertheless, the influence of acquisition settings should not be neglected, as shown by the results provided in this article.

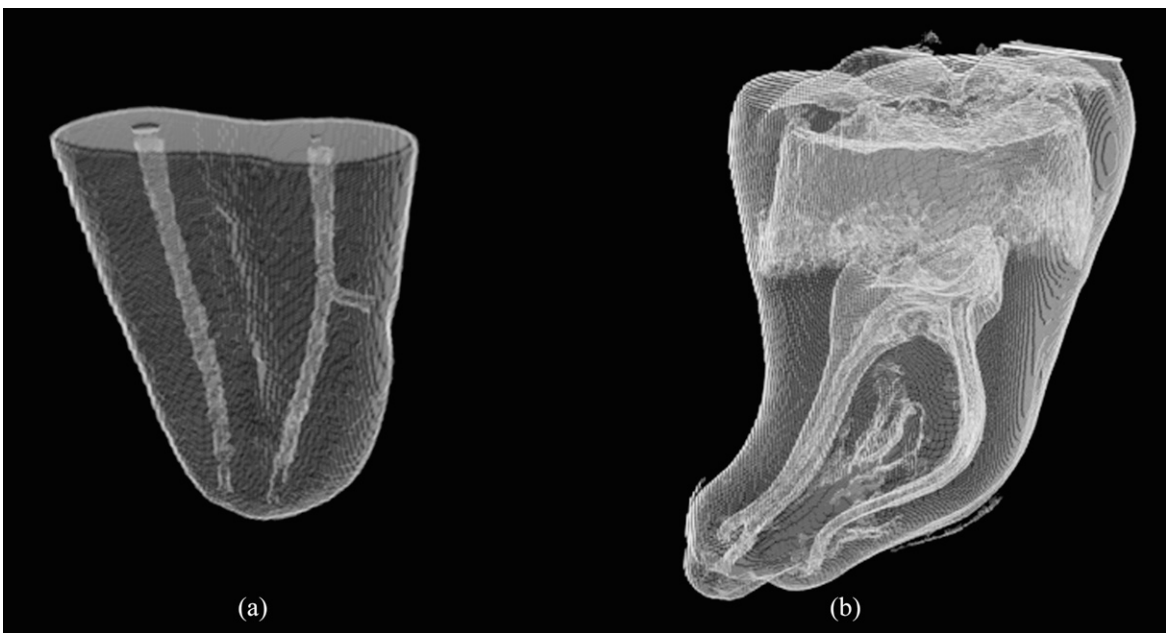

Figure 7 Output three-dimensional images of the edge-detection module: maxillary premolar sample (a) and intact mandibular molar (b).

References

1. Peters OA. Current challenges and concepts in the preparation of root canal systems: a review. *J Endod* 2004; **30**: 559–67. doi: 10.1097/01.DON.0000129039.59003.9D
2. Scarfe WC, Levin MD, Gane D, Farman AG. Use of cone beam computed tomography in endodontics. *Int J Dent* 2009; **2009**: 634567. doi: 10.1155/2009/634567
3. Nemtoi A, Czink C, Haba D, Gahleitner A. Cone beam CT: a current overview of devices. *Dentomaxillofac Radiol* 2013; **42**: 20120443. doi: 10.1259/dmfr.20120443
4. Michetti J, Maret D, Mallet JP, Diemer F. Validation of cone-beam computed tomography as a tool to explore root canal anatomy. *J Endod* 2010; **36**: 1187–90. doi: 10.1016/j.joen.2010.03.029
5. Gonzalez RC, Woods RE. *Digital image processing*. 3rd edn. Pearson International Edition. New Jersey, NJ: Pearson Prentice Hall; 2008.
6. Esposito SA, Huybrechts B, Slagmolen P, Cotti E, Coucke W, Pauwels R, et al. A novel method to estimate the volume of bone defects using cone-beam computed tomography: an *in vitro* study. *J Endod* 2013; **39**: 1111–15. doi: 10.1016/j.joen.2013.04.017
7. Maret D, Telmon N, Peters OA, Lepage B, Treil J, Inglèse JM, et al. Effect of voxel size on the accuracy of 3D reconstructions with cone beam CT. *Dentomaxillofac Radiol* 2012; **41**: 649–55. doi: 10.1259/dmfr/81804525
8. Kato A, Ohno N. Construction of three-dimensional tooth model by micro-computed tomography and application for data sharing. *Clin Oral Investig* 2009; **13**: 43–6. doi: 10.1007/s00784-008-0198-4
9. Hangartner TN. Thresholding technique for accurate analysis of density and geometry in QCT, pQCT and μCT images. *J Musculoskelet Neuronal Interact* 2007; **7**: 9–16.
10. Waarsing JH, Day JS, Weinans H. An improved segmentation method for *in vivo* microCT imaging. *J Bone Miner Res* 2004; **19**: 1640–50. doi: 10.1359/JBMR.040705
11. Hassan B, Couta Souza P, Jacobs R, de Azambuja Berti S, van der Stelt P. Influence of scanning and reconstruction parameters on quality of three-dimensional surface models of the dental arches from cone beam computed tomography. *Clin Oral Investig* 2010; **14**: 303–10. doi: 10.1007/s00784-009-0291-3
12. Kwong JC, Palomo JM, Landers MA, Figueroa A, Hans MG. Image quality produced by different cone-beam computed tomography settings. *Am J Orthod Dentofacial Orthop* 2008; **133**: 317–27. doi: 10.1016/j.ajodo.2007.02.053
13. Hawkes DJ. Algorithms for radiological image registration and their clinical application. *J Anat* 1998; **193**: 347–61. doi: 10.1046/j.1469-7580.1998.19330347.x
14. Hassan BA, Payam J, Juyanda B, van der Stelt P, Wesselink PR. Influence of scan settings on root canal visibility with cone beam CT. *Dentomaxillofac Radiol* 2012; **41**: 645–8. doi: 10.1259/dmfr/27670911
15. Martin CJ, Sharp PF, Sutton DG. Measurement of image quality in diagnostic radiology. *Appl Radiat Isot* 1999; **50**: 21–38. doi: 10.1016/S0969-8043(98)00022-0
16. Bamba J, Araki K, Endo A, Okano T. Image quality assessment of three cone beam CT machines using the SEDENTEXCT CT phantom. *Dentomaxillofac Radiol* 2013; **42**: 201220445. doi: 10.1259/dmfr.20120445
17. Panmekiate S, Apinhasmit W, Petersson A. Effect of electric potential and current on mandibular linear measurements in cone beam CT. *Dentomaxillofac Radiol* 2012; **41**: 578–82. doi: 10.1259/dmfr/51664704
18. Gündoğdu S, Mahmutyazicioğlu K, Ozdemir H, Savranlar A, Asil K. Assessment of image quality of a standard and three dose-reducing protocols in adult cranial CT. *Eur Radiol* 2005; **15**: 1959–68.
19. Katsumata A, Hirukawa A, Okumura S, Naitoh M, Fujishita M, Ariji E, et al. Effects of image artifacts on gray-value density in limited-volume cone-beam computerized tomography. *Oral Surg Oral Med Oral Pathol Oral Radiol Endod* 2007; **104**: 829–36. doi: 10.1016/j.tripleo.2006.12.005
20. Scherf H, Tilgner R. A new high-resolution computed tomography (CT) segmentation method for trabecular bone architectural analysis. *Am J Phys Anthropol* 2009; **140**: 39–51. doi: 10.1002/ajpa.21033
21. Gao Y, Peters OA, Wu H, Zhou X. An application framework of three-dimensional reconstruction and measurement for endodontic research. *J Endod* 2009; **35**: 269–74. doi: 10.1016/j.joen.2008.11.011
22. Loubele M, Jacobs R, Maes F, Denis K, White S, Coudyzer W, et al. Image quality *vs* radiation dose of four cone beam computed tomography scanners. *Dentomaxillofac Radiol* 2008; **37**: 309–18. doi: 10.1259/dmfr/16770531
23. Liu Y, Olszewski R, Alexandroni ES, Enciso R, Xu T, Mah JK. The validity of *in vivo* tooth volume determinations from cone-beam computed tomography. *Angle Orthod* 2010; **80**: 160–6. doi: 10.2319/121608-639.1